CANFSA

Center for Advanced Non-Ferrous Structural Alloys

An Industry/University Cooperative Research Center

Project 37b-L: Rationalization of Liquid/Solid and Solid/Solid Interface Instabilities During Thermal-Mechanical Transients of Metal Additive Manufacturing (ISU)

Summer 2020 Videoconference

June 29 – July 1, July 8 – 10 2020

- ISU team: Katie O'Donnell, Matt Kenney, Maria Quintana
- Faculty: Dr. Peter Collins (ISU)
- MURI members: S. Babu (UTK), A. Clark (CSM), J. R. Jinschek (OSU), T. Pollock (UCSB), Z. Kong (VT), S. Ringer and X. Liao (Univ. of Sydney), S. Primig (Univ. of South Wales) and TEAM
- Industrial Mentors: Billy Short and Jennifer Wolk (ONR)

NSF | COLORADO SCHOOL OF MINES | IOWA STATE UNIVERSITY

Project 37b-L: Rationalization of Liquid/Solid and Solid/Solid Interface Instabilities During Thermal-Mechanical Transients of Metal Additive Manufacturing (ISU)

CANFSA
CENTER FOR ADVANCED NON-FERROUS STRUCTURAL ALLOYS

- ISU team: Matt Kenney, Katie O'Donnell, Maria Quintana
- Advisor(s): Prof. Peter Collins (ISU)

Project Duration
August 2018 to August 2021

- Problem: Understand the thermal gradients in an AM build as a function of different scan strategies by studying the microstructure.
- Objective: To understand the science behind the relation between thermal gradients and the microstructure and texture evolution.
- Benefit: Optimize the final cost and mechanical properties of the AM component.

Recent Progress

- New Ti64 samples are being EDM cut
- Continuing development of an Atlas for defects
- EBSD around selected defects (in progress)
- EDS analysis around selected defects (in progress)
- Preparation of papers for publication

Metrics		
Description	**% Complete**	**Status**
1. Sample preparation for optical, SEM-BSE, EBSD and TEM	50%	● (green)
2. Literature review	60%	● (green)
3. Texture scans – EBSD,SRAS, and ASTAR PED	50%	● (green)
4. 3D analysis	10%	● (yellow)
5. Relate thermal gradients to microstructure and the final mechanical properties	20%	● (red)

Industrial Relevance

- Understanding underlying behavior of different AM strategies on resulting microstructure and mechanical properties of metallic printed parts
- Build a scientific basis into Integrated Computational Materials Engineering (ICME) predictions of AM knowledge gap areas (nano and micro scale regimes of length and time)
- Reduce trial and error phase of AM design and manufacture curve

Progress

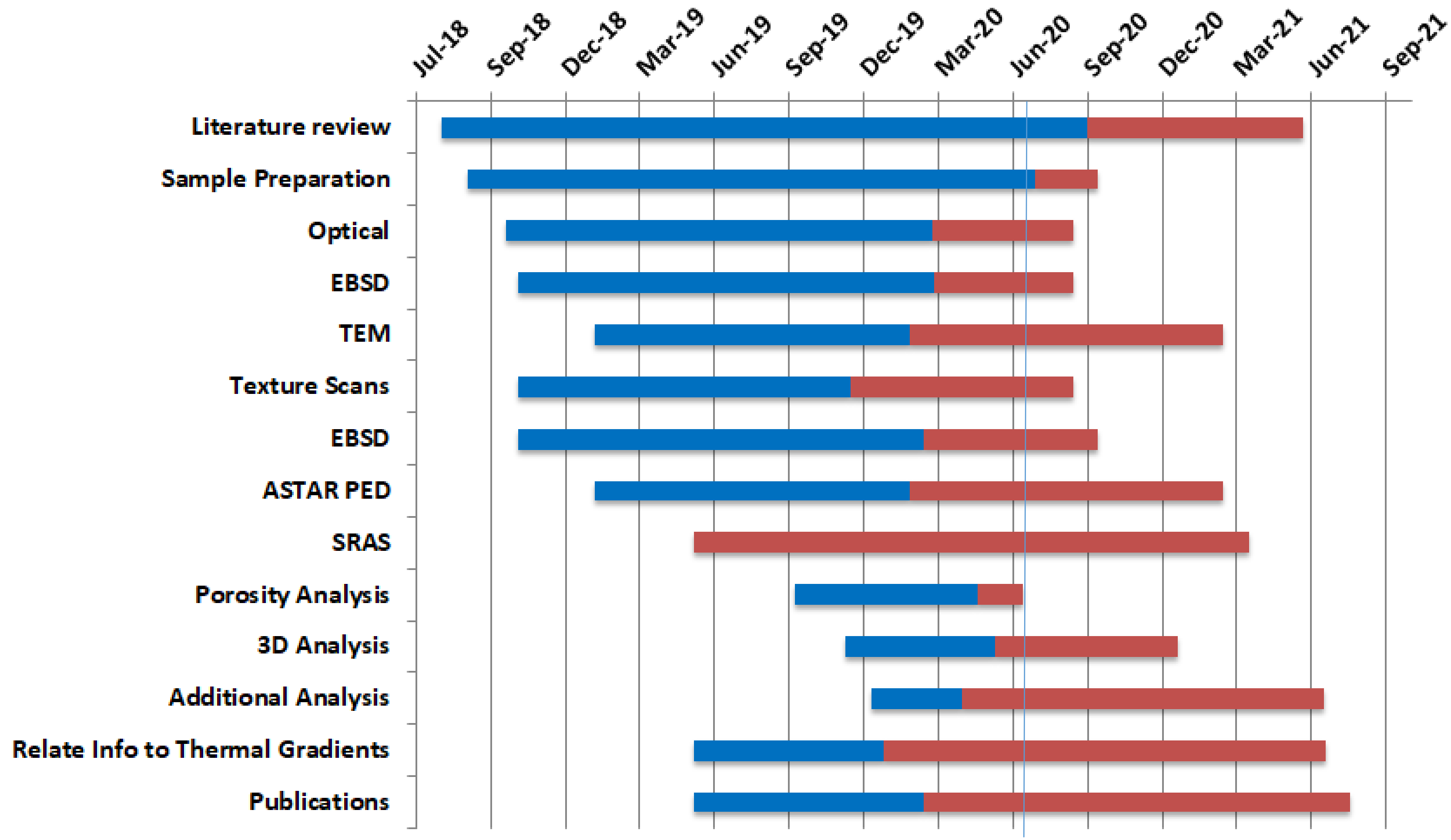
Jul-18
Sep-18
Dec-18
Mar-19
Jun-19
Sep-19
Dec-19
Mar-20
Jun-20
Sep-20
Dec-20
Mar-21
Jun-21
Sep-21
Literature review
Sample Preparation
Optical
EBSD
TEM
Texture Scans
EBSD
ASTAR PED
SRAS
Porosity Analysis
3D Analysis
Additional Analysis
Relate Info to Thermal Gradients
Publications

Research Interests

- Three different AM scan strategies are selected to understand fundamental research questions. The different scan strategies will change the thermal gradient: Raster, Dehoff, and Random

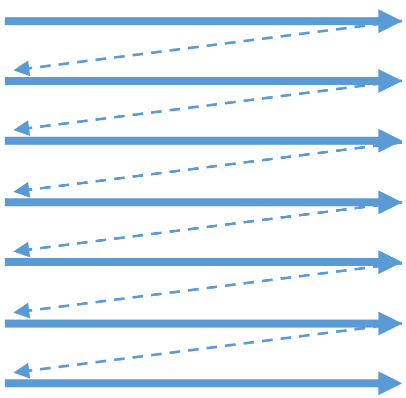

Ordering of Raster Fill

Ordering of Dehoff Fill

Ordering of Random Fill

Outline of the Project

- Ti64 AM and Inconel 738 builds with different scan strategies are provided by ONRL – Raster(L), Random (R) and Dehoff (D)

- **TASKS:**
- Imaging – Macro, Optical and SEM-BSE

1. Texture (across length scales)
   A. SRAS – Spatially Resolved Acoustic Spectroscopy (macro-texture)
   B. EBSD – Electron Back Scattered Diffraction (SEM) (micro-texture)
   C. PED – Precession Electron Diffraction (TEM) (nano-texture)
2. Analysis of the 2D and 3D data
3. Develop the understanding to relate thermal gradient to the microstructural evolution

Material

- 3 cuboid Ti64 AM builds – Raster (L5), Random (R5), and Dehoff (D5)
- 2 cuboid Inconel 738 builds – Random and Raster
- Z is the build direction for all the samples
- 3 new Ti64 samples – cube, pyramid, spiral

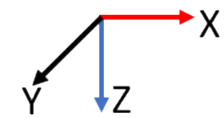

Raster (L5)

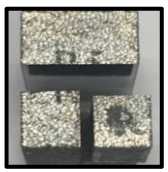

Random (R5)

Dehoff (D5)

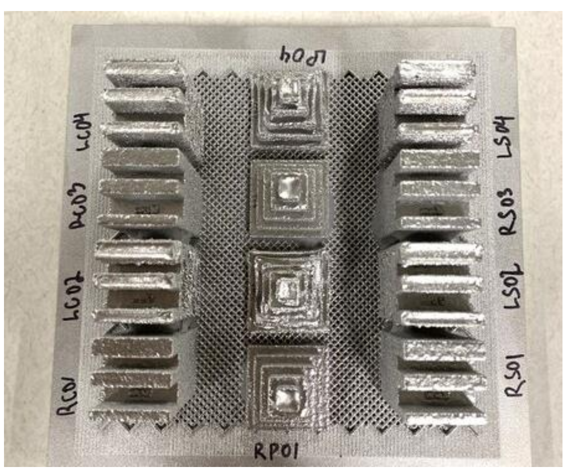

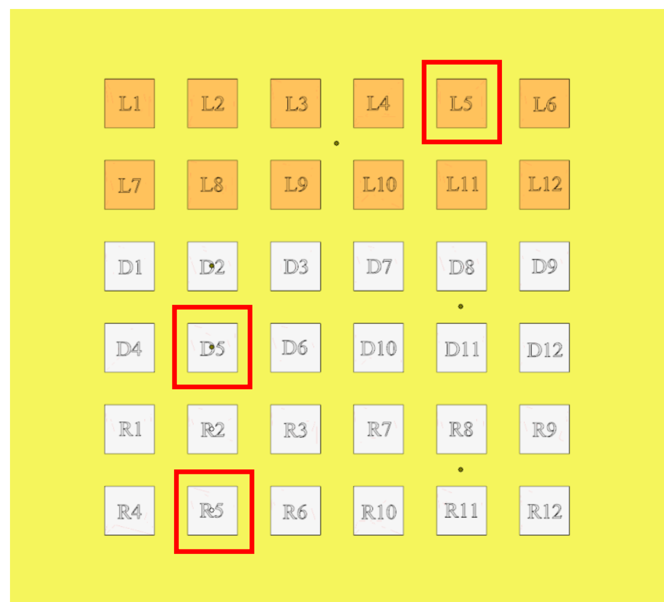

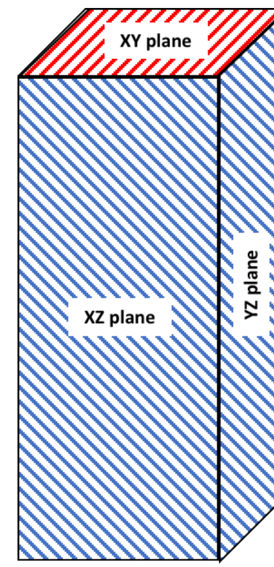

15x15x25mm

Defect Atlas Update

- An attempt to catalogue the first and second order characteristics present in AM defects in order to relate them back to local thermomechanical gyrations within a build

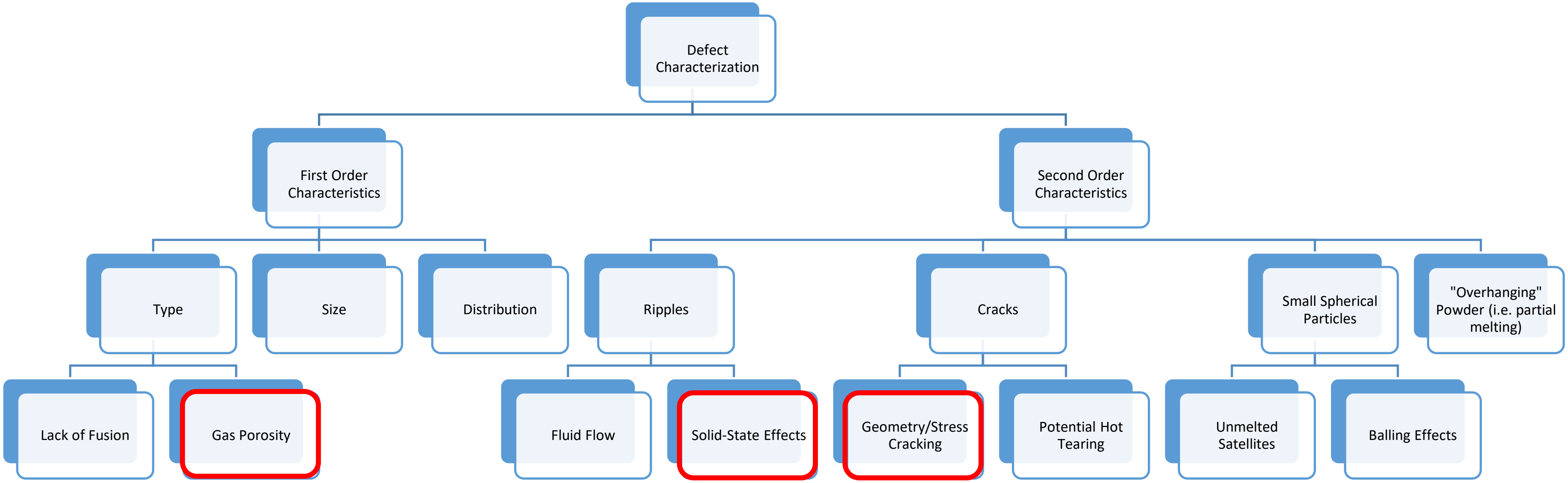

- Other factors to consider:
  - Grain growth around defects/local microstructure
  - Contamination (build plate contamination)

Spherical Porosity: Distribution and Size

- Range of equivalent diameters: approximately 7-37 µm, in eight measured pores from optical mosaics of one-half cut/polished XZ-plane
- Six spherical pores were observed in the L5 sample, and one spherical pore apiece in the R5 and D5 samples
- Consistent with OSU data of porosity in powder:
  - Mean pore size: 10.43 µm
  - Range: 4.08 - 34.51 µm

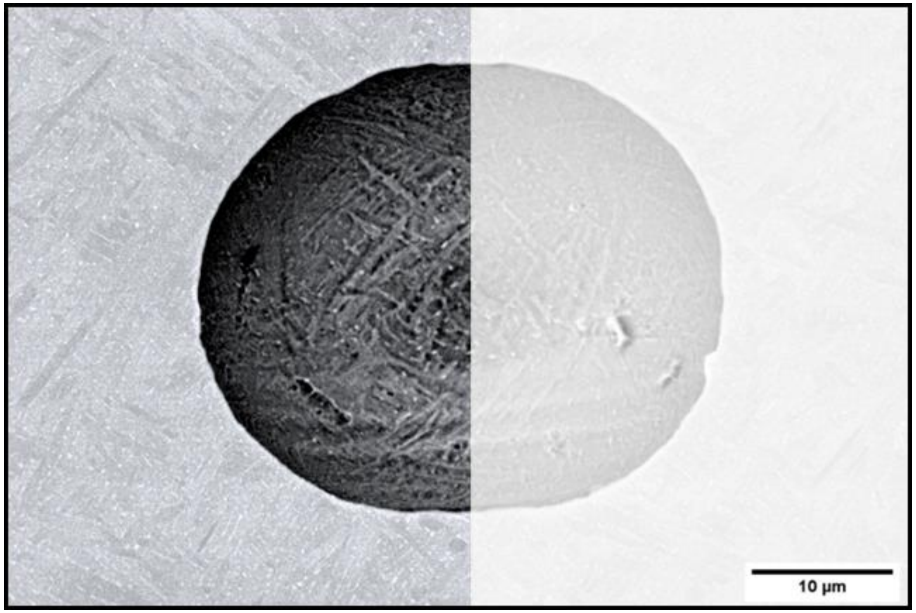

Spherical Porosity: Retained Gas Porosity

CANFSA
CENTER FOR ADVANCED NON-FERROUS STRUCTURAL ALLOYS

- Hypothesis:
  - Spherical porosity is retained gas porosity from argon entrapped within the powder
  - Spot melting scan strategies more easily allow gas bubbles to escape, as opposed to the raster scan strategy
    - i.e. different shapes of the melt pool/varying thermal gyrations effects entrapment of gas porosity

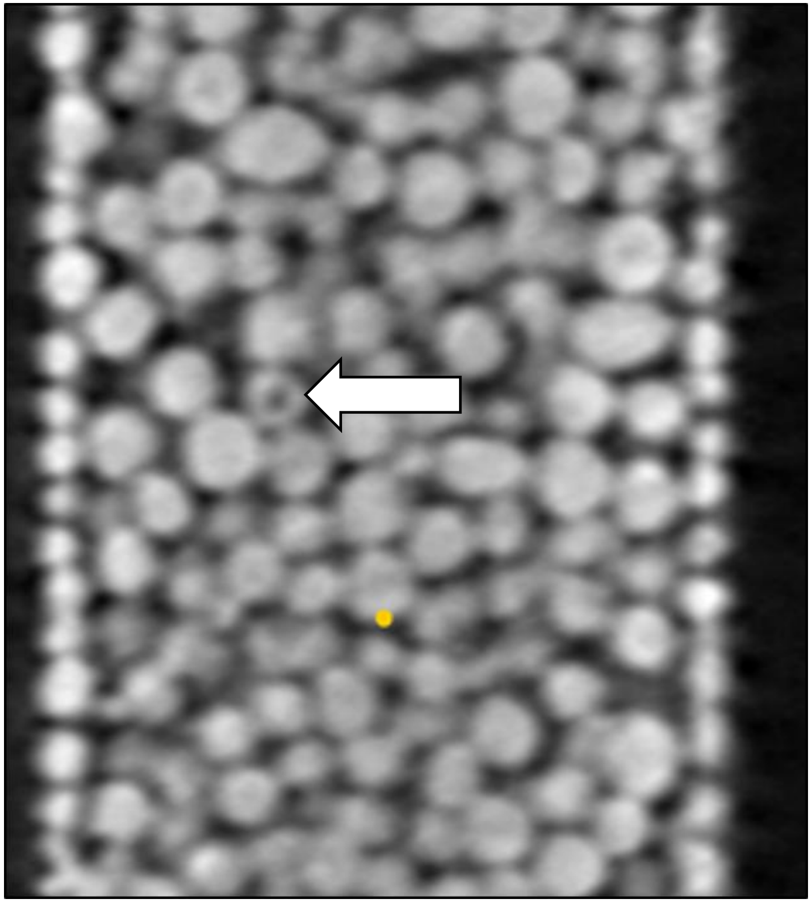

Spherical Porosity Distribution:
Literature Review

- Competing fluid flow forces: gravity, buoyancy, drag, and Marangoni convection
- Hojjatzadeh et al. defines three regions in a raster melt pool – circulation, transition, and laser interaction
  - Ratio of Marangoni convection to drag forces is highest in the laser interaction region (gravity and buoyancy are usually considered negligible in comparison)

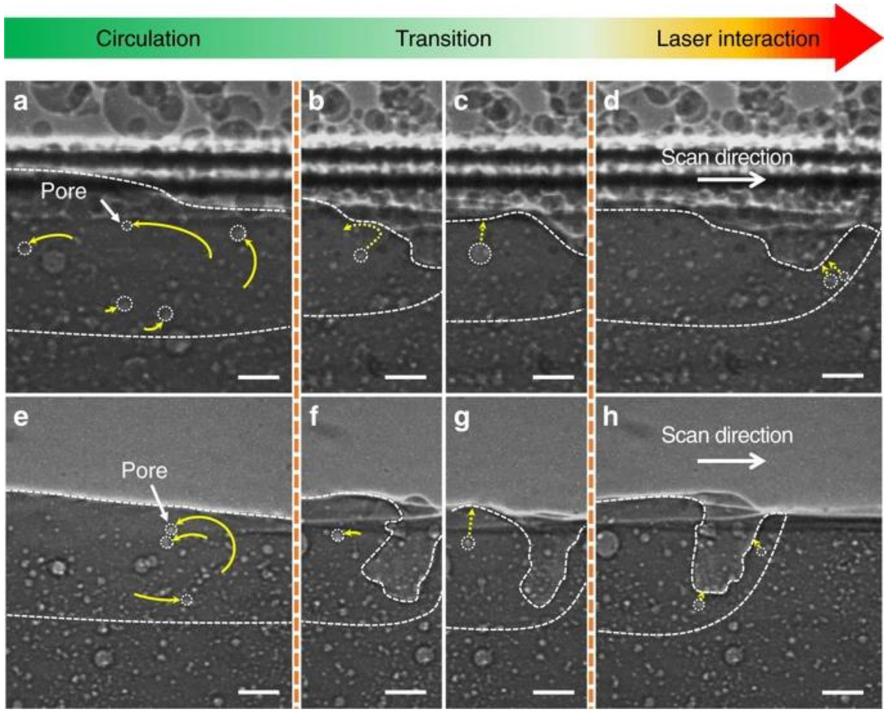

Spherical Porosity Distribution:
LITERATURE REVIEW

- Spherical pores are most able to escape the melt pool in the laser interaction region - i.e. the more Marangoni convection dominates fluid flow
  - Hypothesis: the spot melting strategy creates melt pools that largely consist of only these "laser interaction domains", without the tail ends seen in raster melt pools, more easily allowing entrapped gas bubbles to escape the melt pool

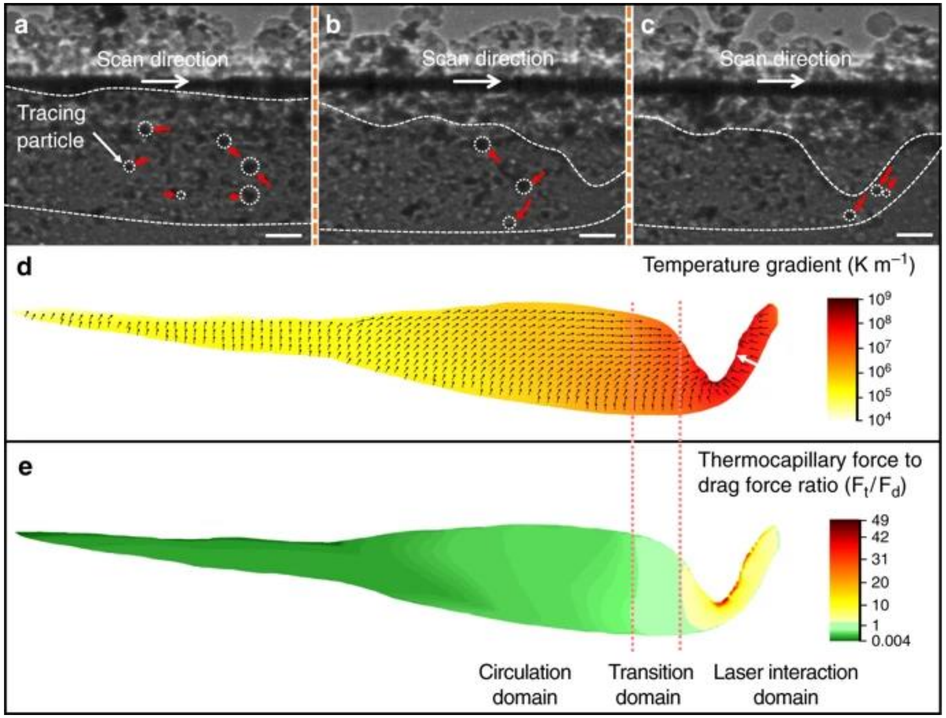

Spherical Porosity:
Horizontal Banding

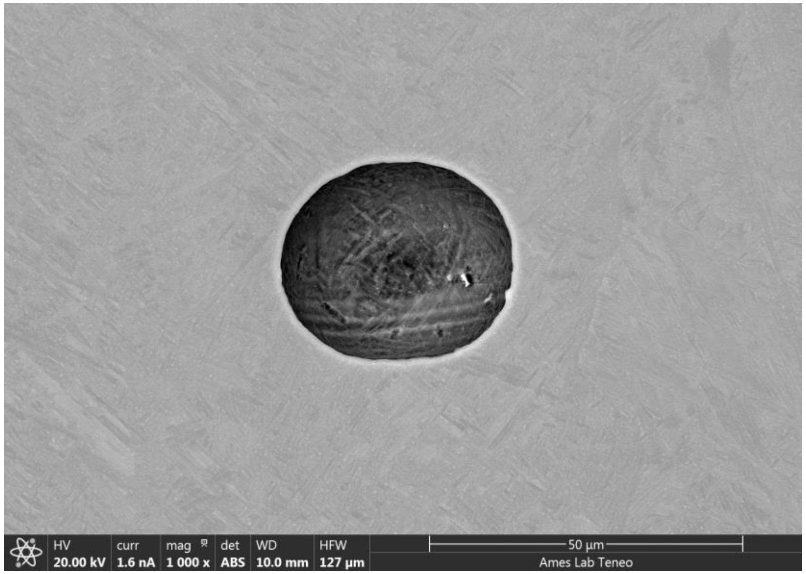

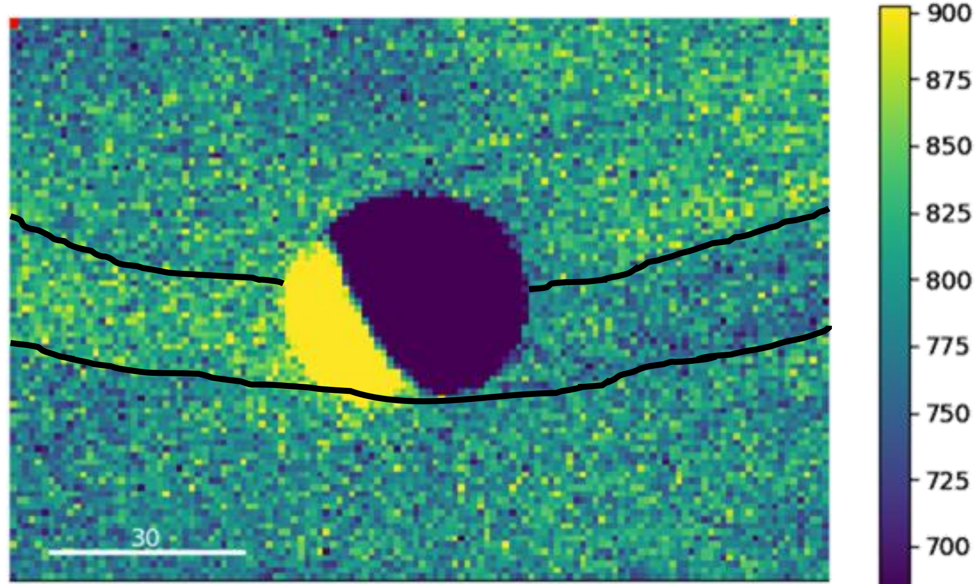

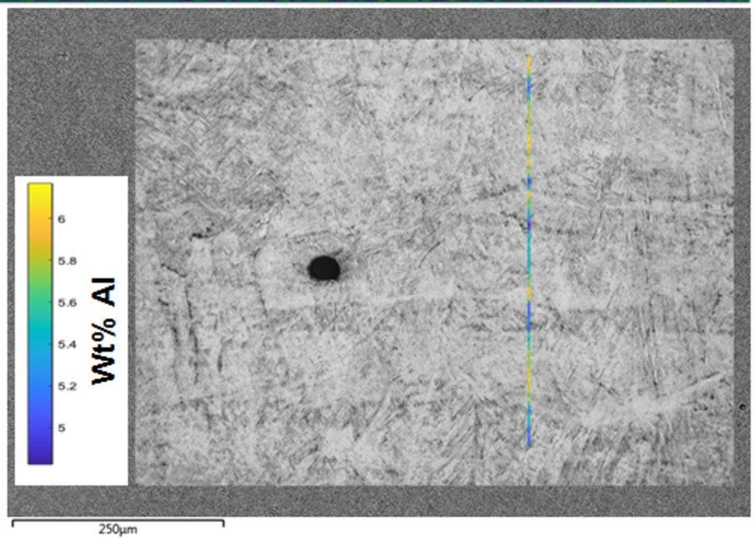

- Visible banding in BSE image (~5µm) is not the same as...
- Compositional fluctuations in EDS map (~20µm) which is approximately the same as...
- Optical banding from Robo-Met.3D® mosaic

Spherical Porosity:

HORIZONTAL BANDING AND ECCENTRICITY

- Banding may be present from accommodation of vertical stresses applied to the pore
- Stresses (solidification?) present during AM process cause the existing spherical pore to become compressed in the Z direction of the build
- The surrounding material then prevents expansion in the X direction which causes buckling in the internal free volume of the pore

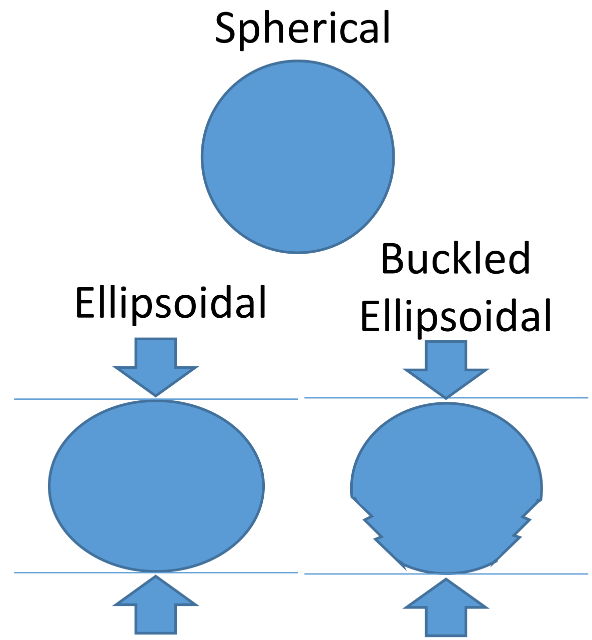

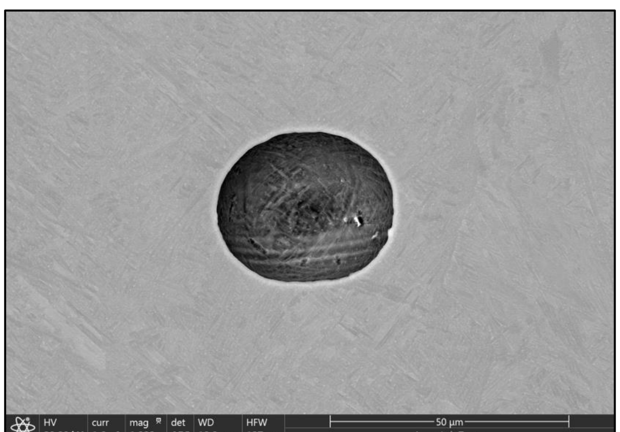

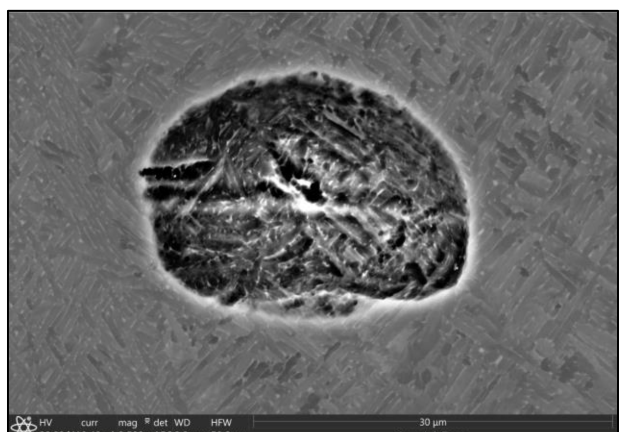

Spherical Porosity:
EBSD

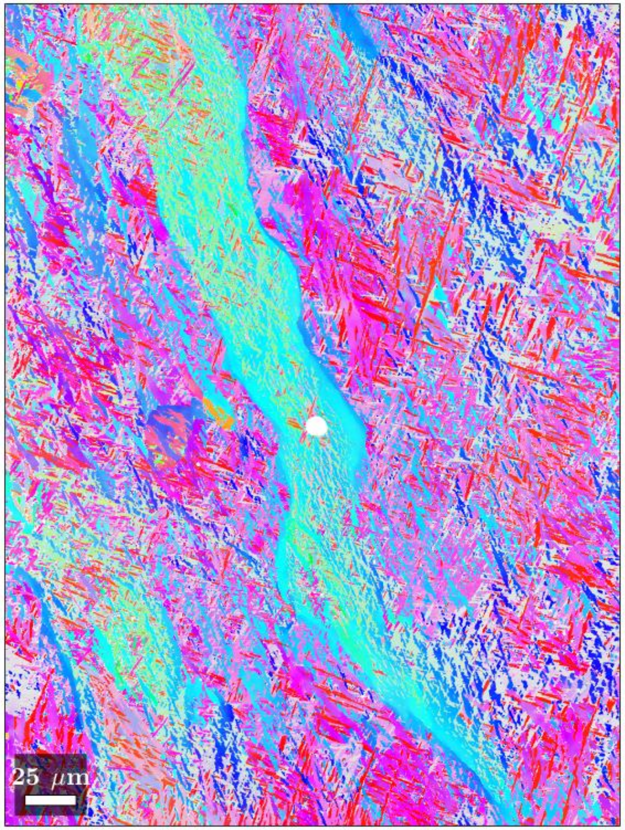

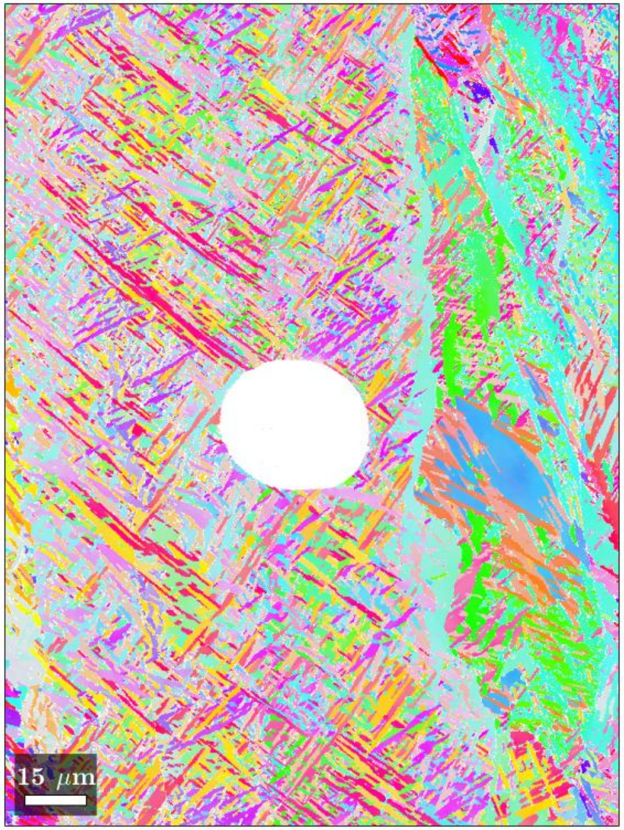

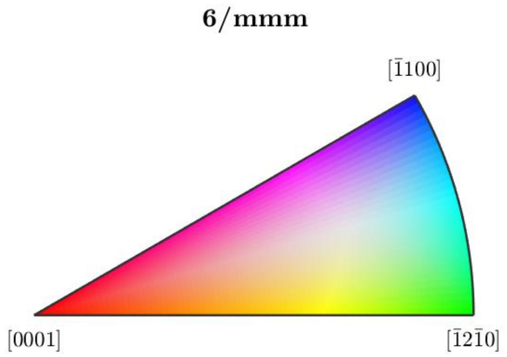

Local Microstructure: Grain Growth Around Defects

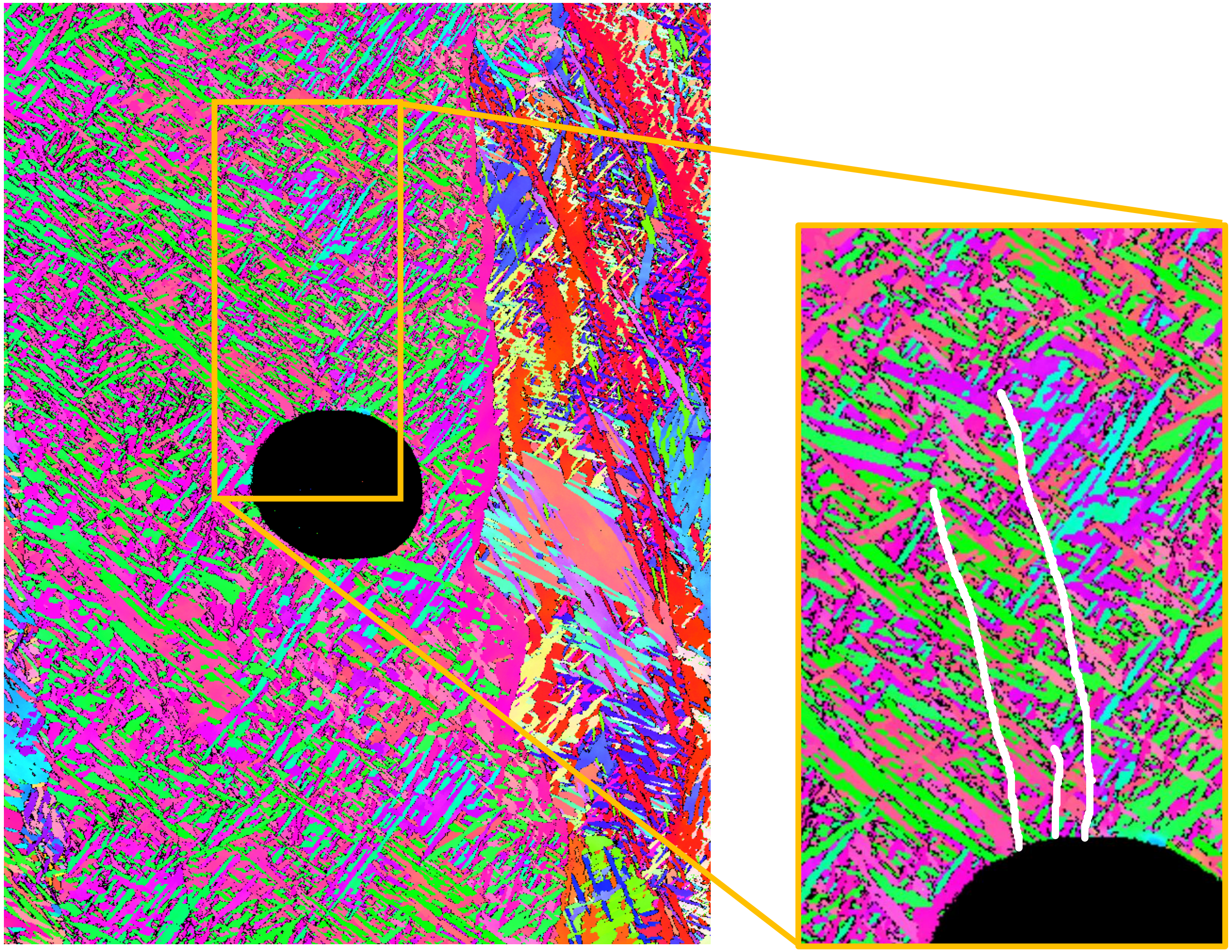

- Evidence of solidification enveloping spherical porosity
- Evidence of small discontinuities on the top side of the pore

Secondary Characteristics: Solid-State Effects

- Free surfaces of pores exhibit structures that could be indicative of fluid flow or solid-state effects
  - Determining the source of such structures has the potential to inform us of local temperature variations and thus local TMGs

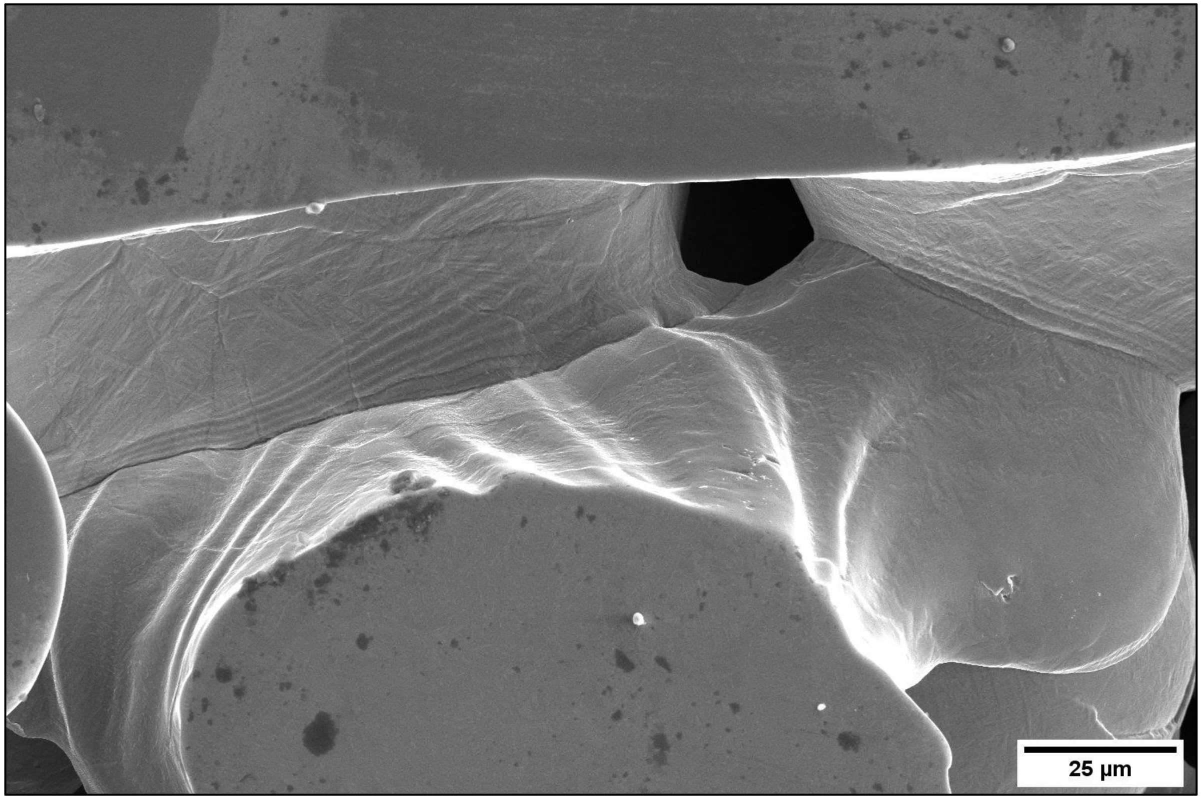

Solid-State Effects:
LITERATURE REVIEW

- Terrace-Ledge-Kink Model
  - Relates crystal growth to energy of an atom in accordance to its bonds with other atoms
    - i.e., the addition of atoms to locations known as kinks does not change the number of corner site molecules, therefore such structures have a significant number of kinks (equilibrium concentration)
- Other models correlate crystal growth with the presence of dislocations
  - Intersection of single screw dislocation with crystal surface, and other interactions

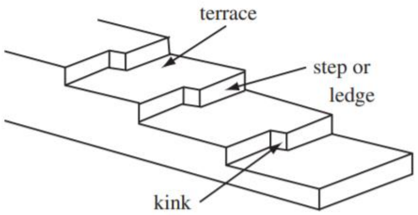

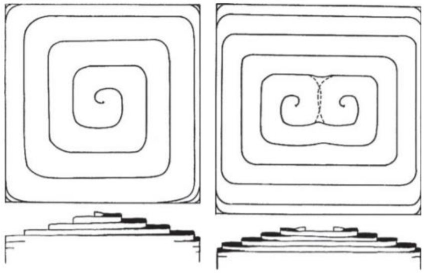

Solid-State Effects:
Sintering Experiment

- Unused Ti-64 powder was wrapped in titanium foil and sealed in two tubes under argon
- Powder was sintered at 925°C and 1025°C for 2 hours

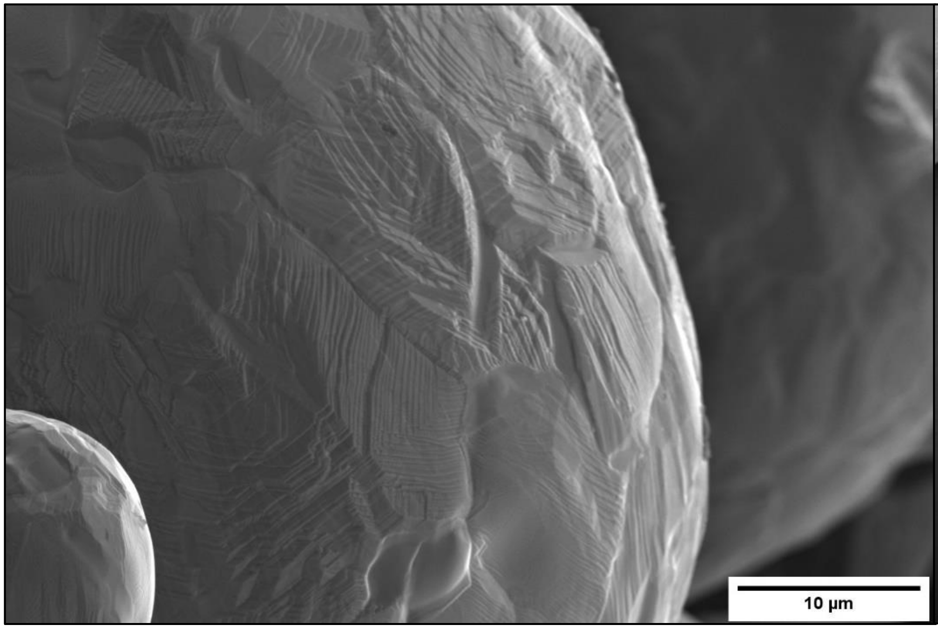

925 °C

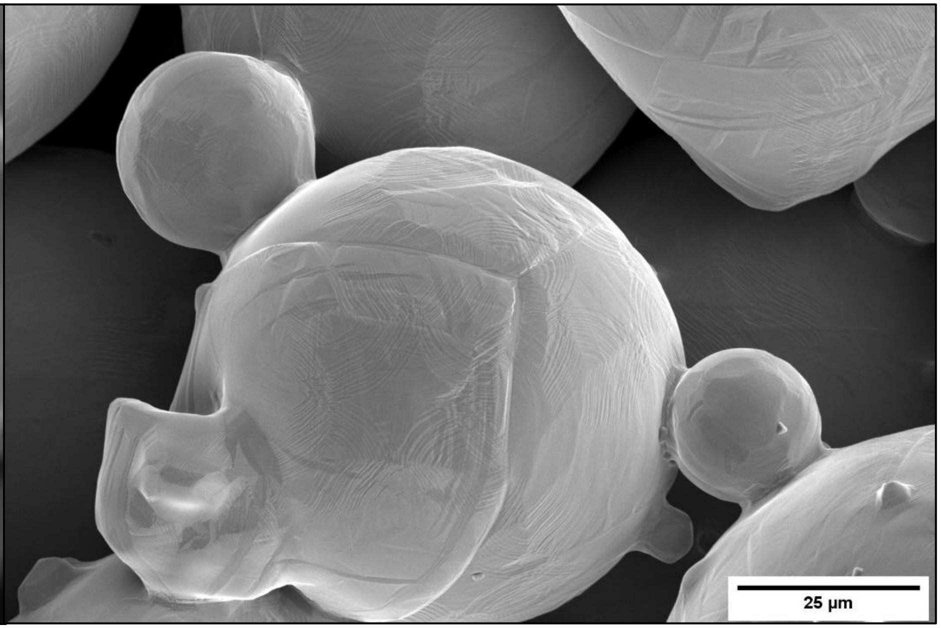

1025 °C

Solid-State Effects:
Sintering Experiment

Floor Ripples: Likely a result of fluid flow

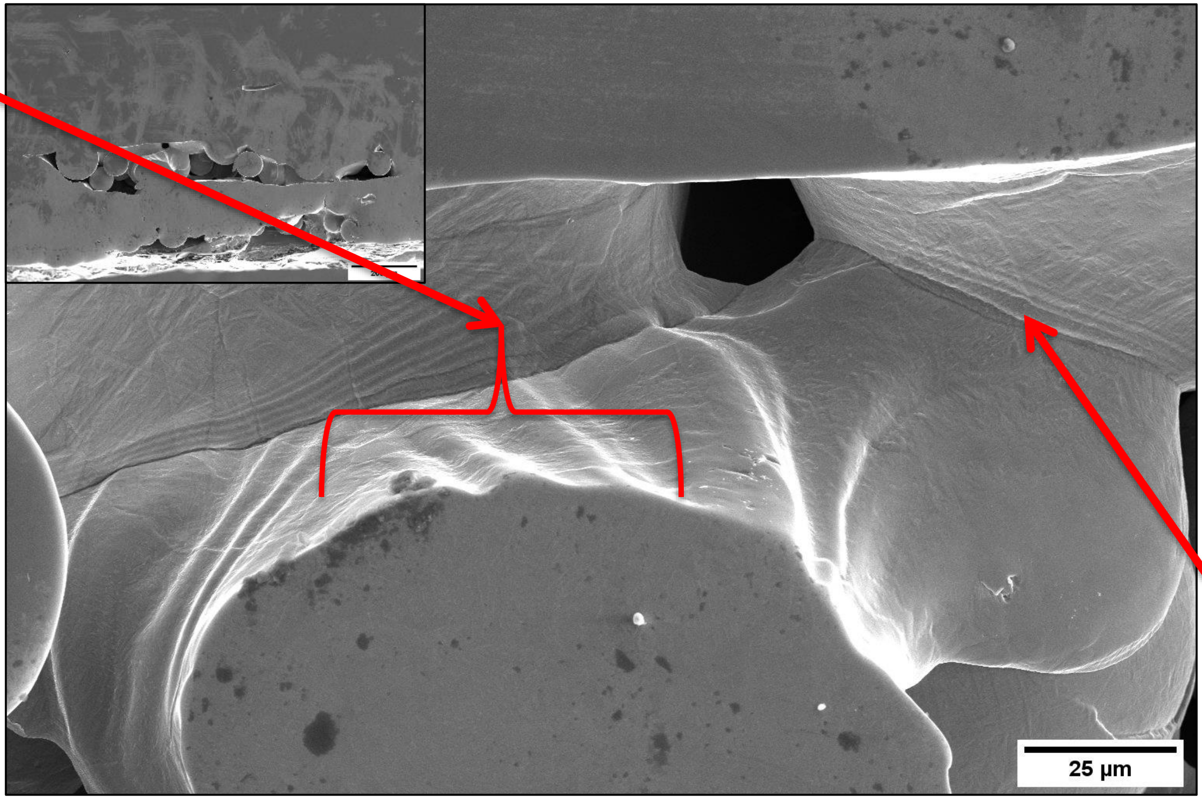

Wall Ripples: Likely a result of solid-state processes

Solid-State Effects:
Thermal Grooving

- Grooves that appear on the surface of polycrystals when heated that coincide with grain boundaries that emerge to intersect the surface
- Three main mechanisms of thermal grooving: evaporation-condensation, surface diffusion, and volume diffusion
  - Surface diffusion is typically dominant when time is small, and can be related back to temperature and time
- Motivation: to relate thermal grooves back to local temperatures/thermal gyrations

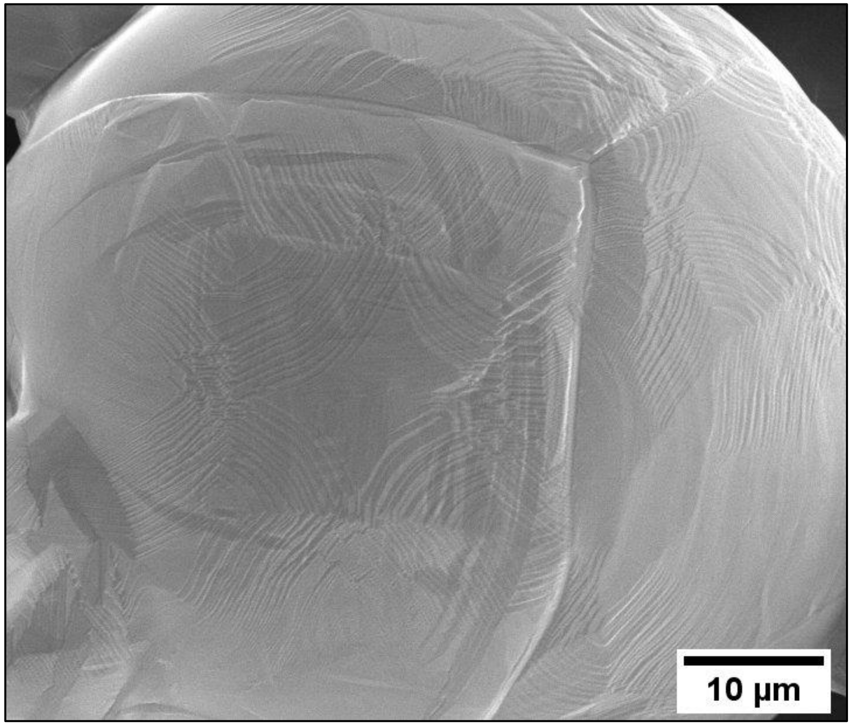

Solid-State Effects:
Thermal Grooving

- Potential Instances of thermal grooving in AM defects:

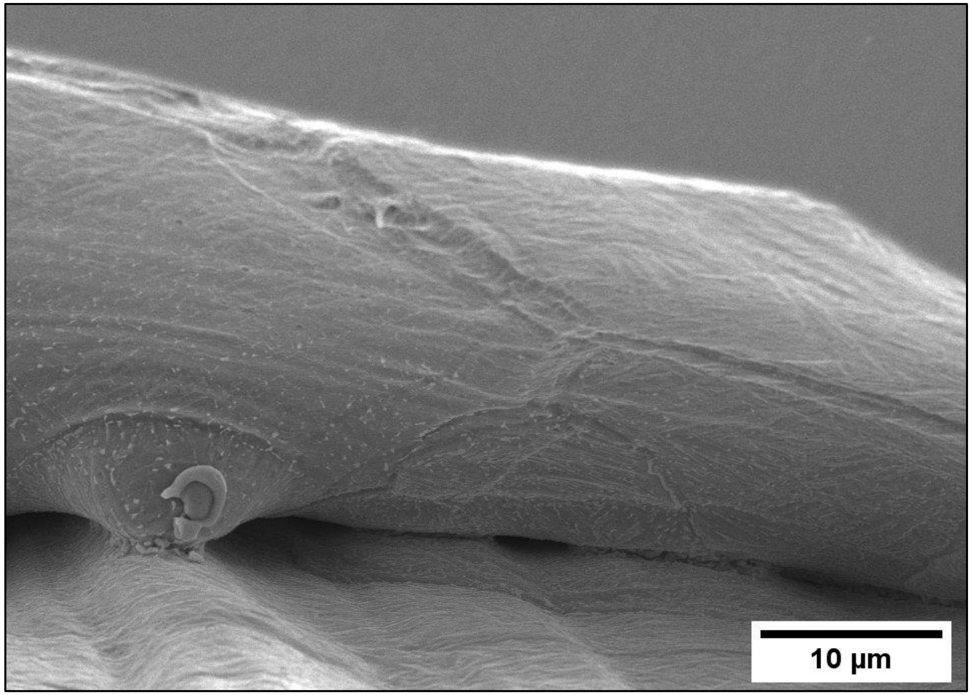

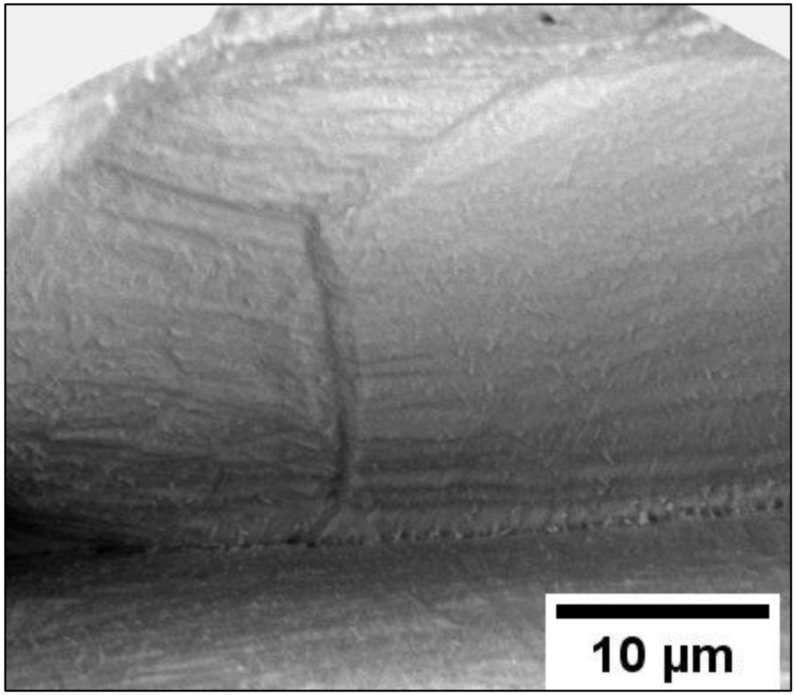

Secondary Characteristics: Geometry/Stress Cracking

CANFSA
CENTER FOR ADVANCED NON-FERROUS STRUCTURAL ALLOYS

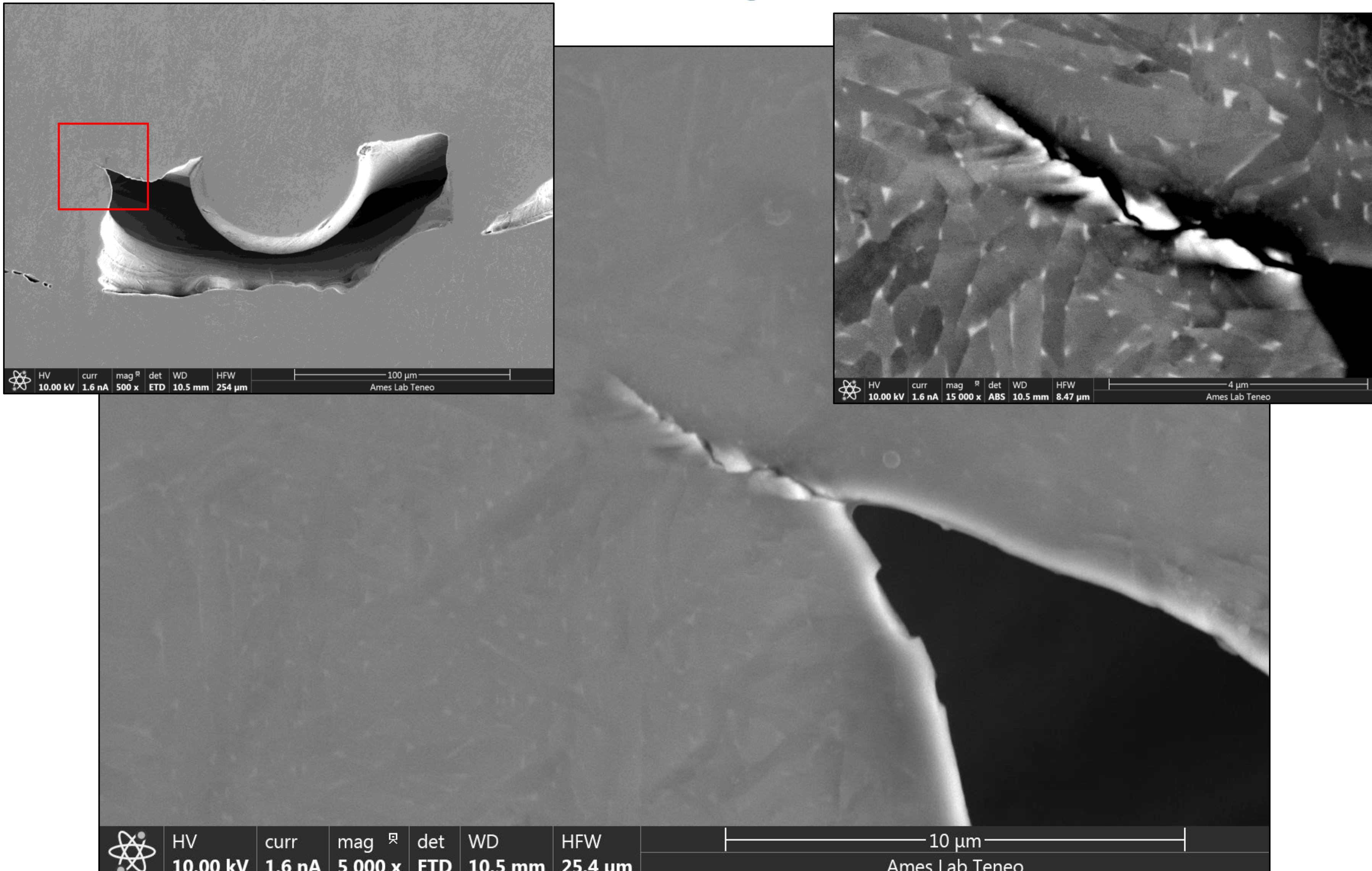

Build Plate Contamination

Bottom of Sample

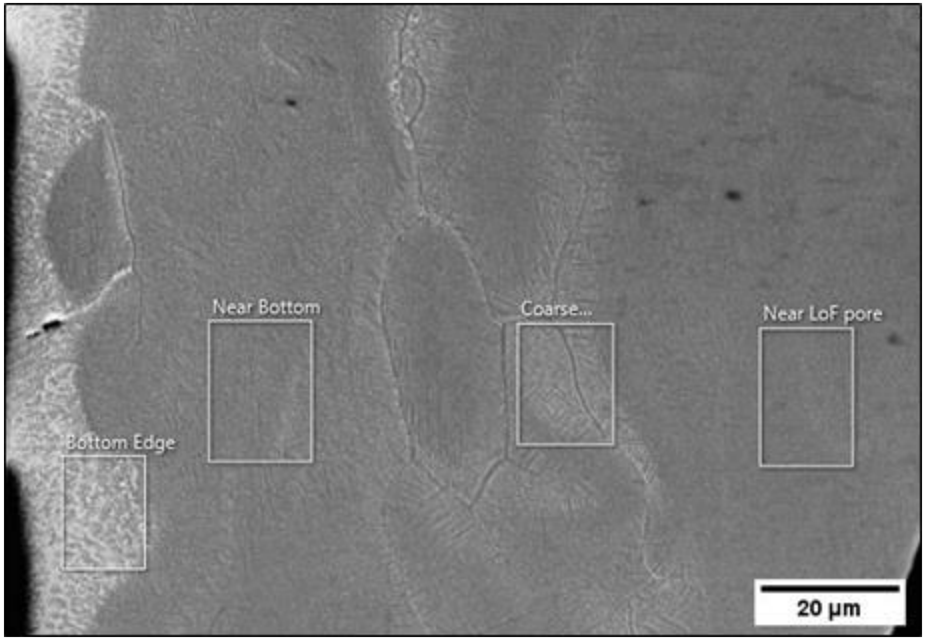

Build Direction →

Area of Interest (L5 sample)	Element (wt%)							
	C	Al	Si	Ti	V	Cr	Fe	Ni
Bottom Edge	2.22	3.48	0.38	70.47	3.09	3.59	14.01	2.76
Near Bottom	2.07	4.54	0.09	86.83	3.99	-	2.12	0.37
Coarse retained beta	2.12	4.21	0.13	85.70	4.12	-	3.21	0.51
Near LoF pore	2.23	4.70	-	88.82	3.69	-	0.56	-
Full View	2.05	4.31	0.11	85.05	4.16	-	3.59	0.73

Build Plate Contamination

Build Direction

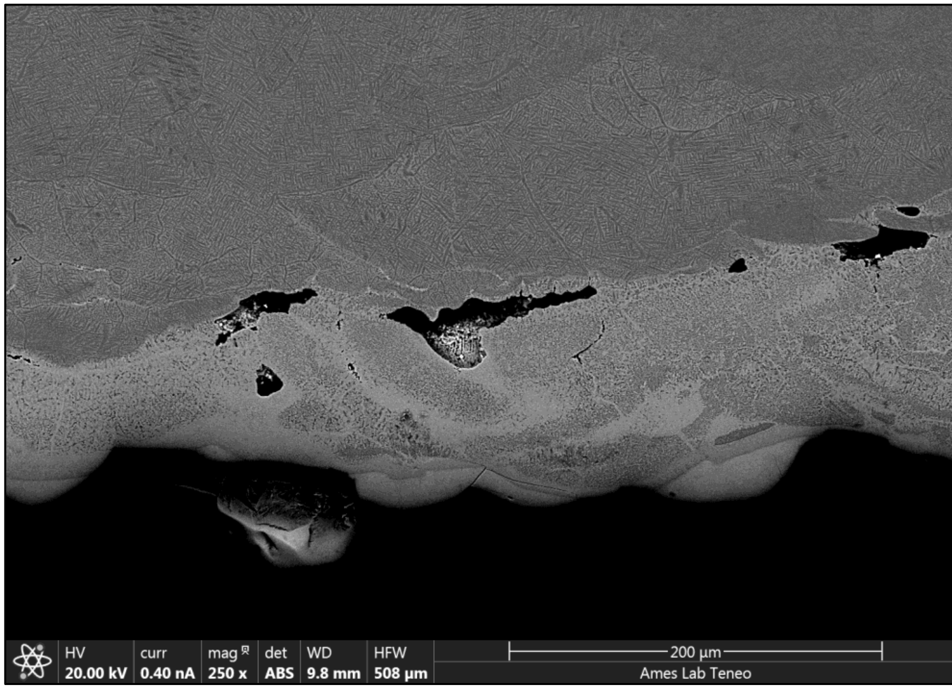

R5

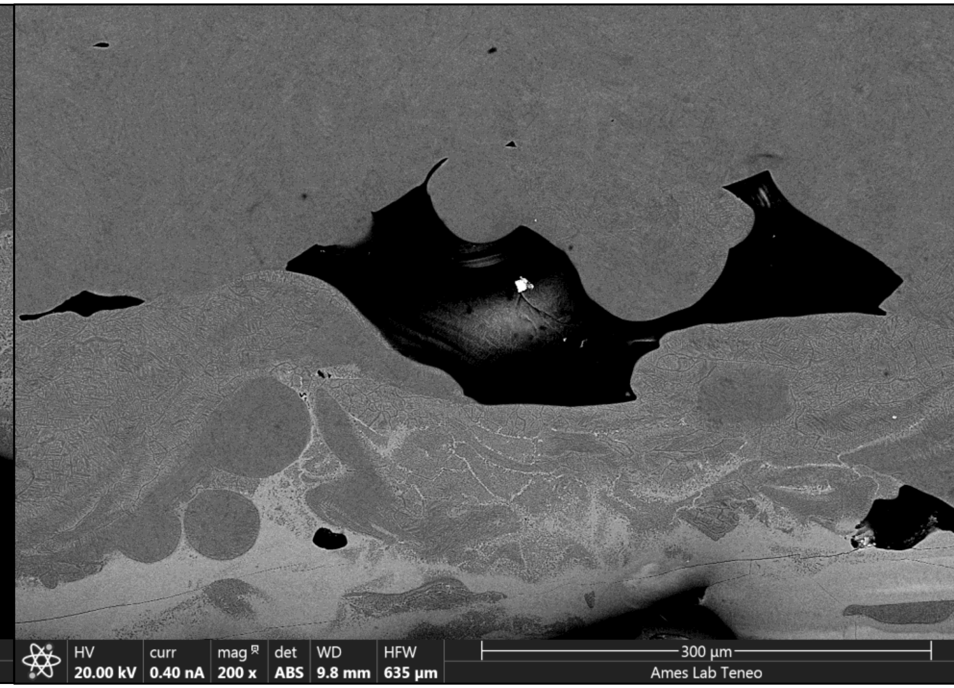

D5

Build Plate Contamination

CANFSA
CENTER FOR ADVANCED
NON-FERROUS STRUCTURAL ALLOYS

Bottom of D5 Sample

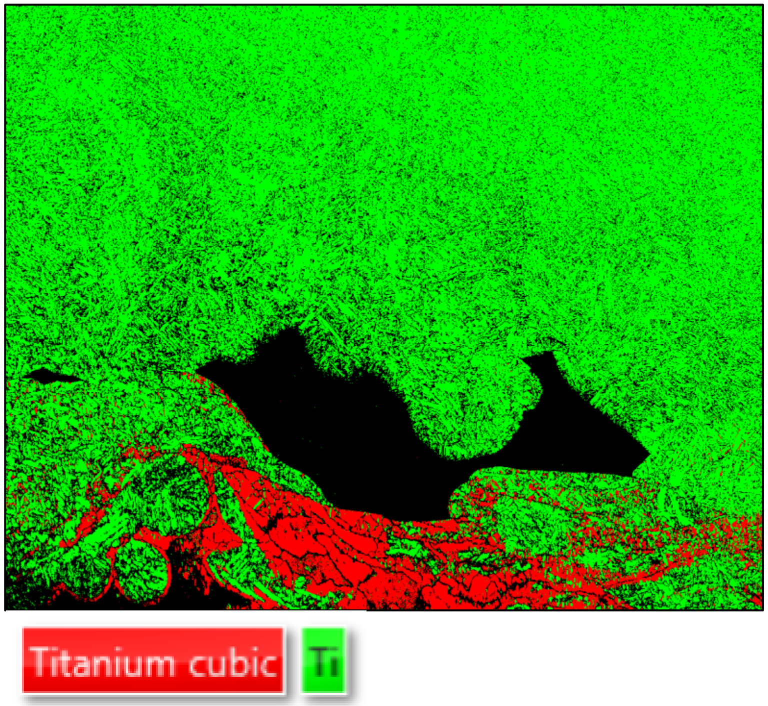

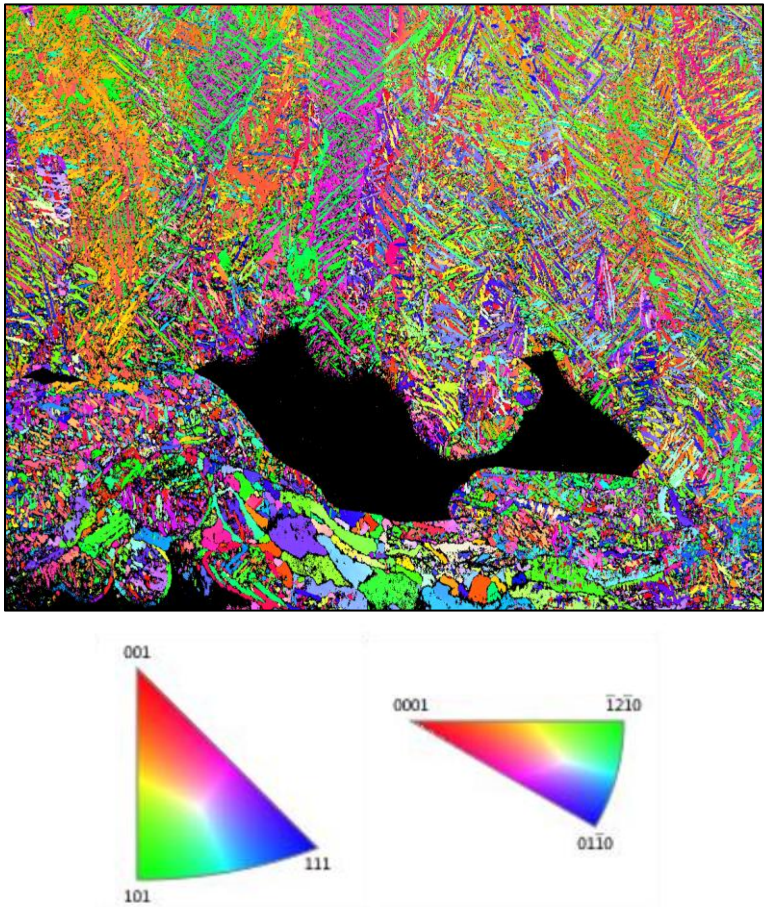

Local Microstructure: Grain Growth Around Defects

CANFSA
CENTER FOR ADVANCED NON-FERROUS STRUCTURAL ALLOYS

- Prior beta grains appear to grow around the large pore at the bottom of the sample
- The large defect acts as a heat flow barrier acting on the surrounding microstructure to change growth direction

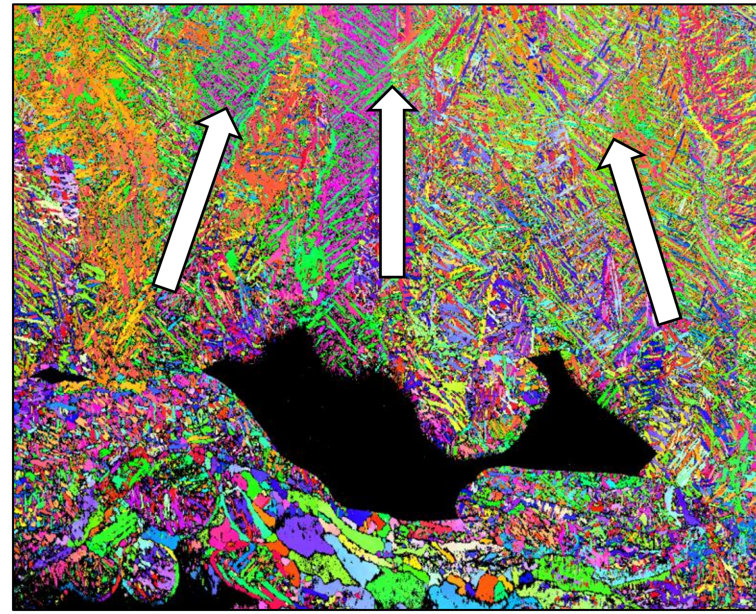

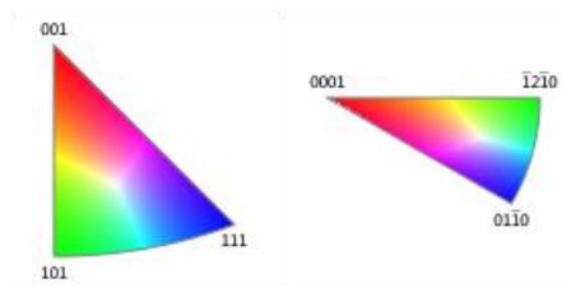

Next Steps

- Spherical Porosity Papers:
  - Observations in spherical porosity
    - Microstructural information around pores (EBSD and EDS analysis)
    - Calculations of eccentricity/sphericity
  - Effect of scanning strategies on the presence of retained gas porosity in EBM
    - Statistical analysis of distribution of spherical pores
- Solid-State effects – analysis of growth ledges; FIB; EBSD
- Stress cracking – FIB liftout near crack; analysis of dislocation density
- Continued defect analysis (Defect Atlas)
- Analysis of new MURI samples

Progress

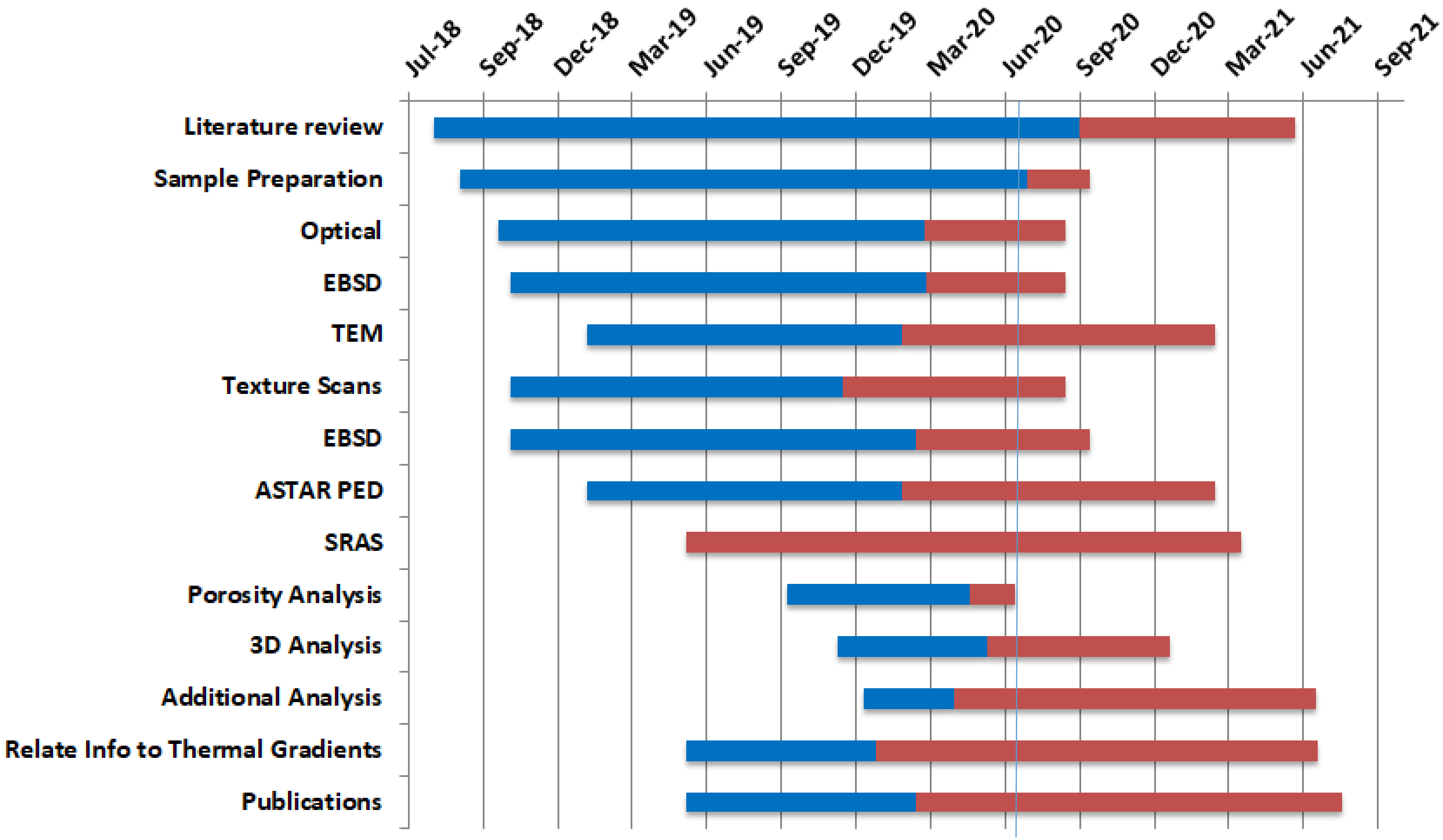
Jul-18
Sep-18
Dec-18
Mar-19
Jun-19
Sep-19
Dec-19
Mar-20
Jun-20
Sep-20
Dec-20
Mar-21
Jun-21
Sep-21
Literature review
Sample Preparation
Optical
EBSD
TEM
Texture Scans
EBSD
ASTAR PED
SRAS
Porosity Analysis
3D Analysis
Additional Analysis
Relate Info to Thermal Gradients
Publications

Thank you!

Katie O'Donnell
katieo1@iastate.edu

References

[1] Tammas-Williams, S., et al. "XCT analysis of the influence of melt strategies on defect population in Ti–6Al–4V components manufactured by Selective Electron Beam Melting." Materials Characterization 102 (2015): 47-61.

[2] Hojjatzadeh, S. Mohammad H., et al. "Pore elimination mechanisms during 3D printing of metals." Nature communications 10.1 (2019): 1-8.

[3] Woodruff, D. P. "How does your crystal grow? A commentary on Burton, Cabrera and Frank (1951)'The growth of crystals and the equilibrium structure of their surfaces'." *Philosophical Transactions of the Royal Society A: Mathematical, Physical and Engineering Sciences* 373.2039 (2015): 20140230.

[4] Mullins, William W. "Theory of thermal grooving." *Journal of Applied Physics* 28.3 (1957): 333-339.

[5] Mullins, W. W. "The effect of thermal grooving on grain boundary motion." *Acta metallurgica* 6.6 (1958): 414-427.